MANCHESTER 1824
The University of Manchester

The University of Manchester Research

The spin-1/2 and spin-1 quantum J_1-J_1'-J_2 Heisenberg models on the square lattice

Document Version
Accepted author manuscript

Link to publication record in Manchester Research Explorer

Citation for published version (APA):
Bishop, RF., Li, PHY., Darradi, R., & Richter, J. (2008). The spin-1/2 and spin-1 quantum J_1-J_1'-J_2 Heisenberg models on the square lattice. In J. Boronat, GE. Astrakharchik, & F. Mazzanti (Eds.), *Recent Progress in Many-Body Theories: Proceedings of the 14th International Conference, Barcelona, Spain, 16-20 July 2007* (pp. 265-274). (Series on Advances in Quantum Many-Body Theory; Vol. 11). World Scientific Publishing Co. Pte. Ltd.

Published in:
Recent Progress in Many-Body Theories

Citing this paper
Please note that where the full-text provided on Manchester Research Explorer is the Author Accepted Manuscript or Proof version this may differ from the final Published version. If citing, it is advised that you check and use the publisher's definitive version.

General rights
Copyright and moral rights for the publications made accessible in the Research Explorer are retained by the authors and/or other copyright owners and it is a condition of accessing publications that users recognise and abide by the legal requirements associated with these rights.

Takedown policy
If you believe that this document breaches copyright please refer to the University of Manchester's Takedown Procedures [http://man.ac.uk/04Y6Bo] or contact openresearch@manchester.ac.uk providing relevant details, so we can investigate your claim.

OPEN ACCESS

Download date:19. May. 2025

Series on Advances in Quantum Many-Body Theory – Vol. 11

Proceedings of the 14th International Conference

RECENT PROGRESS *in* MANY-BODY THEORIES

Barcelona, Spain 16 – 20 July 2007

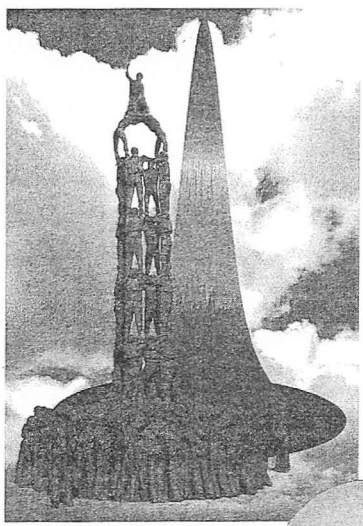

Editors

Jordi Boronat
Gregory E. Astrakharchik
Ferran Mazzanti

Universitat Politècnica de Catalunya
Spain

World Scientific

NEW JERSEY • LONDON • SINGAPORE • BEIJING • SHANGHAI • HONG KONG • TAIPEI • CHENNAI

THE SPIN-1/2 AND SPIN-1 QUANTUM J_1–J_1'–J_2 HEISENBERG MODELS ON THE SQUARE LATTICE

R. F. BISHOP†* and P. H. Y. LI

School of Physics and Astronomy, The University of Manchester, Manchester, M13 9PL, UK

†*E-mail: raymond.bishop@manchester.ac.uk*

R. DARRADI and J. RICHTER

Institut für Theoretische Physik, Otto-von-Guericke Universität Magdeburg, 39016 Magdeburg, Germany

We study the J_1–J_1'–J_2 quantum spin model on the two-dimensional square lattice using the coupled cluster method. We compare and contrast the influence of the interchain coupling J_1' on the zero-temperature phase diagrams for the two spin values $s = 1/2$ and $s = 1$. Our most important result for the $s = 1/2$ case is the predicted existence of a quantum triple point (QTP) at $(J_1' \approx 0.60 \pm 0.03, J_2 \approx 0.33 \pm 0.02)$ when $J_1 = 1$. Below the QTP $(J_1'/J_1 \lesssim 0.60)$ we predict a second-order phase transition between the quasi-classical Néel and stripe-ordered phases, whereas the corresponding classical model, which contains only these two phases for all spin values s, yields a first-order transition. Above the QTP $(J_1'/J_1 \gtrsim 0.60)$ an intermediate disordered phase emerges, which has no classical counterpart. By contrast, the situation for $s = 1$ is qualitatively different. Instead of a QTP where three phases co-exist, we now predict a quantum tricritical point at $(J_1' \approx 0.66 \pm 0.03, J_2 \approx 0.35 \pm 0.02)$ when $J_1 = 1$, where a line of second-order phase transitions between the quasi-classical Néel and stripe-ordered phases (for $J_1'/J_1 \lesssim 0.66$) meets a line of first-order phase transitions between the same two states (for $J_1'/J_1 \gtrsim 0.66$). Surprisingly, we find no evidence at all for any intermediate disordered phase in the $s = 1$ case.

Keywords: J_1–J_1'–J_2 model; coupled cluster method; quantum phase transition; frustrated magnet; spin-lattice system; quantum triple point; quantum tricritical point; spin-half model; spin-one model.

1. Introduction

The frustrated Heisenberg antiferromagnet with nearest-neighbour J_1 and competing next-nearest-neighbour J_2 coupling (J_1–J_2 model) has received renewed interest both theoretically (see Refs. [1–7] and references cited therein) and experimentally[8,9] due to the recent discovery or successful syntheses of such new magnetic materials,

*On sabbatical leave during 2007–08 at William I. Fine Theoretical Physics Institute, School of Physics and Astronomy, University of Minnesota, 116 Church Street S.E., Minneapolis, MN 55455, USA.

as the layered-oxide high-temperature superconductors, whose undoped precursors can be well described by the model. The interplay between frustration and quantum fluctuations in two-dimensional (2D) quantum spin systems can lead to rich and unusual phase scenarios between magnetically ordered semiclassical phases and novel quantum paramagnetic ground state phases (see Ref. [10] and references cited therein). An interesting generalization of the pure J_1–J_2 model has also been introduced recently by Nersesyan and Tsvelik.[11] They consider a 2D spatially anisotropic spin-1/2 J_1–J_1'–J_2 model on the square lattice, where the nearest-neighbour bonds have different strengths J_1 and J_1' in, say, the x (intrachain) and y (interchain) directions respectively. This model has been further studied by other groups using the exact diagonalization (ED) of small lattice samples of $N \leq 36$ sites,[12] and the continuum limit of the model.[13] Both groups support the prediction by Nersesyan and Tsvelik[11] of a resonating valence bond state for $J_2 = 0.5J_1' \ll J_1$, and the limit of small interchain coupling extends along a curve nearly coincident with the line where the energy per spin is maximum. The model has also been studied by Moukouri[14] using a two-step density-matrix renormalization group approach.

Although spin problems are conceptually simple, they often exhibit rich and interesting phase diagrams due to the strong influence of quantum fluctuations in these strongly correlated systems. The strength of the quantum fluctuations can be tuned by varying either the anisotropy terms in the Hamiltonian[15] or the spin quantum number s.[16] Thus, lattice quantum spin problems maintain an important role in the study of quantum phase transitions. Very few calculations have been performed for the J_1–J_1'–J_2 model for the case of $s = 1$ up till now. It has, however, been studied using the two-step density-matrix renormalization group method, but only for the specific value of $J_1'/J_1 = 0.2$, and a second-order transition from a Néel phase to a disordered phase is observed with a spin gap.[6] It has also been observed that quantum fluctuations can destabilize the ordered classical ground state (GS), even for large values of s, for large enough values of the frustration.[1,5]

Furthermore, it has been argued recently that the quantum phase transition between the semiclassical Néel phase and the quantum paramagnetic phase present in the 2D J_1–J_2 model is not described by a Ginzburg-Landau type critical theory, but rather may exhibit a deconfined quantum critical point.[17,18]

The aim of this paper is to further the study of the J_1–J_1'–J_2 model by using the coupled cluster method (CCM). The CCM (and see Refs. [19–21] and references cited therein) is one of the most powerful and universally applicable techniques of quantum many-body theory. It has been applied successfully to calculate with high accuracy the ground- and excited-state properties of many lattice quantum spin systems (and see Refs. [7,21–25] and references cited therein). The CCM is appropriate for studying frustrated systems for which such other methods as quantum Monte Carlo techniques are limited by the infamous minus-sign problem, and exact diagonalization methods are restricted in practice to such small lattices that may be insensitive to the details of the often subtle phase order present.

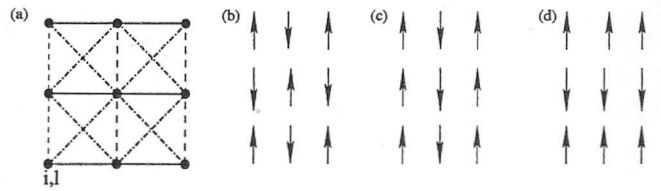

Fig. 1. (a) J_1–J_1'–J_2 model; — J_1; - - - J_1'; - · - J_2; (b) Néel state; (c) stripe state - columnar; and (d) stripe state - row. Arrows in (b), (c), and (d) represent spins situated on the sites of the square lattice (indicated by • in (a)).

2. The Model

The J_1–J_1'–J_2 model is a general spin-s Heisenberg model on a square lattice with three kinds of exchange bonds, with strenth J_1 along the row direction, J_1' along the column direction, and J_2 along the diagonals, as shown in Fig. 1. All exchanges are assumed positive here, and we set $J_1 = 1$. The Hamiltonian of the model is described by

$$H = J_1 \sum_{i,l} \mathbf{s}_{i,l} \cdot \mathbf{s}_{i+1,l} + J_1' \sum_{i,l} \mathbf{s}_{i,l} \cdot \mathbf{s}_{i,l+1} + J_2 \sum_{i,l} (\mathbf{s}_{i,l} \cdot \mathbf{s}_{i+1,l+1} + \mathbf{s}_{i+1,l} \cdot \mathbf{s}_{i,l+1}). \quad (1)$$

This model has two types of classical ground state, namely, the Néel (π, π) state and stripe states (columnar stripe $(\pi, 0)$ and row stripe $(0, \pi)$), the spin orientations of which are shown in Figs. 1(b,c,d) respectively. There is clearly a symmetry under the interchange of rows and columns, $J_1 \rightleftharpoons J_1'$, which implies that we need only consider the range of parameters with $J_1' < J_1$. The ground state energies of the various classical states are given by

$$\begin{aligned} \frac{E^{\rm cl}_{\rm N\acute{e}el}}{N} &= (-J_1 - J_1' + 2J_2)|s|^2, \\ \frac{E^{\rm cl}_{\rm columnar}}{N} &= (-J_1 + J_1' - 2J_2)|s|^2, \\ \frac{E^{\rm cl}_{\rm row}}{N} &= (J_1 - J_1' - 2J_2)|s|^2. \end{aligned} \quad (2)$$

We take $J_1 = 1$ and $J_1' < 1$. Clearly, from Eq. (2), the classical GS is then either the Néel state (if $J_1' > 2J_2$) or the stripe state (if $J_1' < 2J_2$). Hence, the (first-order) classical phase transition between the Néel and stripe (columnar) states occurs at $J_2^c = \frac{1}{2}J_1'$, $\forall J_1 > J_1'$.

3. The Coupled Cluster Method Formalism

The CCM formalism is now briefly described (and see Refs. [19–26] for further details). The starting point for any CCM calculation is to select a normalized model or reference state $|\Phi\rangle$. It is often convenient to take a classical GS as a model state for

CCM calculations of quantum spin systems. Accordingly our model states here are the Néel state and the stripe state. It is very convenient to treat each site on an equal footing, and in order to do so we perform a mathematical rotation of the local axes on each lattice site such that all spins in every reference state align along the negative z-axis. The Schrödinger ground state ket and bra equations are $H|\Psi\rangle = E|\Psi\rangle$ and $\langle\tilde{\Psi}|H = E\langle\tilde{\Psi}|$ respectively. The CCM parametrizes these exact quantum GS wave functions in the forms $|\Psi\rangle = \mathrm{e}^{S}|\Phi\rangle$ and $\langle\tilde{\Psi}| = \langle\tilde{\Phi}|\tilde{S}\mathrm{e}^{-S}$. The correlation operators S and $\tilde{S}$ are expressed as $S = \sum_{I\neq 0} \mathcal{S}_I C_I^+$ and $\tilde{S} = 1 + \sum_{I\neq 0} \tilde{\mathcal{S}}_I C_I^-$, where $C_0^+ \equiv 1$, the unit operator, and $C_I^+ \equiv (C_I^-)^\dagger$ is one of a complete set of multispin creation operators with respect to the model state (with $C_I^-|\Phi\rangle = 0 = \langle\Phi|C_I^+$), generically written as $C_I^+ \equiv s_{i_1}^+ s_{i_2}^+ \cdots s_{i_n}^+$, in terms of the spin-raising operators $s_i^+ \equiv s_i^x + s_i^y$ on lattice sites i.

The ket- and bra-state correlation coefficients $(\mathcal{S}_I, \tilde{\mathcal{S}}_I)$ are calculated by requiring the expectation value $\bar{H} \equiv \langle\tilde{\Psi}|H|\Psi\rangle$ to be a minimum with respect to each of them. This immediately yields the coupled set of equations $\langle\Phi|C_I^-\mathrm{e}^{-S}H\mathrm{e}^{S}|\Phi\rangle = 0$ and $\langle\Phi|\tilde{S}(\mathrm{e}^{-S}H\mathrm{e}^{S} - E)C_I^+|\Phi\rangle = 0\,;\,\forall I \neq 0$, which we solve for the correlation coefficients $(\mathcal{S}_I, \tilde{\mathcal{S}}_I)$. We may then calculate the GS energy from the relation $E = \langle\Phi|\mathrm{e}^{-S}H\mathrm{e}^{S}|\Phi\rangle$, and the GS staggered magnetization M from the relation $M \equiv -\frac{1}{N}\langle\tilde{\Psi}|\sum_{i=1}^{N} s_i^z|\Psi\rangle$ which holds in the rotated spin coordinates. We note that we work from the outset in the $N \to \infty$ limit.

4. Approximation Schemes

The CCM formalism is exact if a complete set of multispin configurations $\{I\}$ with respect to the model state is included in the calculation. However, it is necessary in practice to use approximation schemes to truncate the expansions in configurations $\{I\}$ of the correlation operators S and $\tilde{S}$. For the case of $s = 1/2$ we employ here, as in our previous work,[7,20–25] the localized LSUBn scheme in which all possible multi-spin-flip correlations over different locales on the lattice defined by n or fewer contiguous lattice sites are retained. The numbers of such fundamental configurations (*viz.*, those that are distinct under the symmetries of the Hamiltonian and of the model state $|\Phi\rangle$) that are retained for the Néel and stripe states of the current model in various LSUBn approximations are shown in Table 1.

We note next that the number of fundamental LSUBn configurations for $s = 1$ becomes appreciably higher than for $s = 1/2$, since each spin on each site i can now be flipped twice by the spin-raising operator s_i^+. Thus, for the $s = 1$ model it is more practical to use the alternative SUBn–m scheme, where m is the size of the locale on the lattice and n is the maximum number of spin-flips. Hence all correlations involving up to n spin flips spanning a range of no more than m adjacent lattice sites are retained.[21,26] In our case we set $m = n$, and hence employ the SUBn–n scheme. More generally, the LSUBm scheme is thus equivalent to the SUBn–m scheme for $n = 2sm$. Hence, LSUB$m \equiv$ SUB$2sm$–m. For $s = 1/2$, LSUB$n \equiv$ SUBn–n; whereas for $s = 1$, LSUB$n \equiv$ SUB$2n$–n. The numbers of fundamental configurations retained

Table 1. Numbers of fundamental configurations (♯ f.c.) for $s = 1/2$ and $s = 1$ in various CCM approximations.

$s = 1/2$			$s = 1$		
Scheme	♯ f.c.		Scheme	♯ f.c.	
	Néel	stripe		Néel	stripe
LSUB2	2	1	SUB2–2	2	1
LSUB4	13	9	SUB4–4	28	21
LSUB6	146	106	SUB6–6	744	585
LSUB8	2555	1922	SUB8–8	35629	29411
LSUB10	59124	45825	–	–	–

at various SUBn–n levels for the $s = 1$ model are shown in Table 1.

In order to solve the corresponding coupled sets of CCM bra- and ket-state equations we use parallel computing.[27,28]

5. Extrapolation Schemes

In practice one needs to extrapolate the raw LSUBn or SUBn–n data to the $n \to \infty$ limit. Based on our previous experience[7,23,25] we use the following empirical three-parameter scaling laws for the extrapolations of the GS energy,

$$E = a_0 + a_1 n^{-2} + a_2 n^{-4} , \tag{3}$$

and of the GS staggered magnetization for frustrated models,

$$M = b_0 + b_1 n^{-\nu} , \tag{4}$$

where the exponent ν is also a fitting parameter.

We list below three fundamental rules, also based on our experience, as guidelines for the selection and extrapolation of the CCM raw data, using *any* approximation scheme.

- Rule 1: As a fundamental rule of numerical fitting or numerical analysis, one should always have at least $(n + 1)$ data points in order to have a robust and stable fit to any formula that contains n unknown parameters. This rule takes precedence over all other rules.
- Rule 2: Whenever possible one should avoid using the lowest (*e.g.*, LSUB2, SUB2-2) data points since such points are rather far from the large-n limit, unless it is necessary to do so to avoid breaking Rule 1.
- Rule 3: If Rule 2 has been broken then some other careful consistency checks should also be performed.

In our results below the LSUBn results for $n = \{4, 6, 8, 10\}$ are extrapolated for $s = 1/2$, in order to preserve the above three rules, whereas the SUBn–n results for $n = \{2, 4, 6, 8\}$ are extrapolated for $s = 1$, in each case using the schemes indicated above. For both the $s = 1/2$ and the $s = 1$ models we perform two separate sets

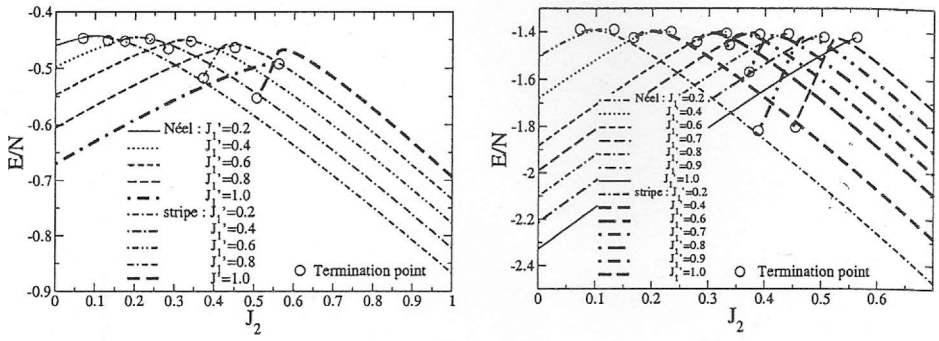

Fig. 2. Ground state energy per spin, E/N (with $J_1 = 1$): (a) for $s = 1/2$; and (b) for $s = 1$.

of CCM calculations for given parameters $(J_1 \equiv 1, J_1', J_2)$ based respectively on the Néel state and the stripe state as the model state $|\Phi\rangle$.

6. Results and Discussion

Figure 2 shows the GS energy per spin as a function of J_2 for various values of J_1' (all with $J_1 \equiv 1$), extrapolated from both the $s = 1/2$ and $s = 1$ models from the raw CCM data as discussed above. Both the raw LSUBn data for the $s = 1/2$ model and the raw SUBn–n data for the $s = 1$ model terminate at some particular values. This occurs for the CCM curves based on both the Néel state and the stripe state as the model state $|\Phi\rangle$. In all cases such a termination point arises due to the solutions of the CCM equations becoming complex at this point, beyond which there exist two branches of complex-conjugate solutions. In the region where the solution reflecting the true physical situation is real, there actually also exists another real solution. However, only the (shown) upper branch of these two solutions reflects the true physical situation, whereas the lower branch does not. The branch reflecting the true physical situation of the solutions is the one which becomes exact in some appropriate (*e.g.*, perturbative) limit. This physical branch then meets the corresponding unphysical branch at some termination point beyond which no real solutions exist. The termination points shown in Fig. 2 are the extrapolated $n \to \infty$ termination points and are evaluated using data only up to the highest level of the CCM approximation schemes used here, namely LSUB10 for the $s = 1/2$ model and SUB8–8 for the $s = 1$ model. The SUBn–n and LSUBn termination points are also reflections of phase transitions in the real system, as we discuss more fully below.

We observe from Fig. 2 that for the case of the $s = 1/2$ model the two curves, based on the Néel and stripe model states, for a given value of J_1', cross (or, in the limit, meet) very smoothly near their maxima for all values of $J_1' \lesssim 0.6$, at a value of J_2 slightly larger than the classical transition point of $0.5J_1'$. This behaviour is indicative of a second-order quantum phase transition between these two phases, by contrast with the first-order classical transition from Eq. (2). Conversely, for values

$J_1' \gtrsim 0.6$ the curves no longer cross at a physical value (*viz.*, where the calculated staggered magnetization is positive), indicating the opening up of an intermediate quantum phase between the Néel and stripe phases. For the case of $s = 1$, the extrapolated GS energy curves of the Néel and stripe states again meet smoothly with the same slope for $J_1' \lesssim 0.66 \pm 0.03$. This behaviour is again indicative of a second-order phase transition. By contrast, for $J_1' \gtrsim 0.66 \pm 0.03$ the behaviour is typical of a first-order phase transition where the curves now cross with a discontinuity in the slope. Figure 2 clearly shows the distinct differences in the GS energy curves for the two models with $s = 1/2$ and $s = 1$. This different behaviour observed in the GS energy for the two models is reinforced by the GS staggered magnetization results discussed below.

For the GS staggered magnetization for the $s = 1/2$ model we find that the extrapolation of Eq. (4) produces smooth and physically reasonable results, except for a very narrow anomalous "shoulder" region near the points where M vanishes for $0.6 \lesssim J_1' \lesssim 0.75$ for the Néel state. This critical regime is undoubtedly difficult to fit with the simple two-term scheme of Eq. (4). Our method for curing this problem and for stabilizing the curves is to make efficient use of the information we obtain in Eq. (4) to extract the exponent ν, and then to use that value to infer the next term in the series. We find, very gratifyingly, that the value for ν fitted to Eq. (4) turns out to be very close to 0.5 for all values of J_1' and J_2 except very close to the critical point. Therefore, we use the form of Eq. (5),

$$M = c_0 + n^{-0.5}\left(c_1 + c_2 n^{-1}\right) . \tag{5}$$

The use of Eq. (5) removes the anomalous shoulder. Henceforth, in all of the results we discuss, we use Eq. (5) for the staggered magnetization.

We have also checked that for the $s = 1/2$ model the extrapolated results using the data sets with $n = \{2, 4, 6, 8, 10\}$ and $n = \{4, 6, 8, 10\}$ are very similar, thereby adding credence to the validity and stability of our results. Conversely, the results using the data set with $n = \{6, 8, 10\}$ again display a minor spurious "shoulder" which is almost certainly due to violating our Rule 1.

For the $s = 1$ model, no narrow anomalous "shoulder" region is observed in the raw SUBn–n results. We have also performed some vigorous tests in the extrapolation schemes for the staggered magnetization in this case. Our main finding is that Eq. (5) using the data set with $n = \{2, 4, 6, 8\}$ is the most consistent in terms of both the GS energy meeting point and the staggered magnetization critical point, as discussed below.

Figure 3 shows our extrapolated results for the GS staggered magnetization M for both models. The quantum phase transition or critical point marking the end of either the quantum Néel state or the quantum stripe state is determined by calculating the order parameter M for various values of J_1' to obtain those values of J_2 where M vanishes. However, as seen in Fig. 3, there also occur cases where the order parameters of the two states meet before the order parameter vanishing point. In these cases we take the meeting point to define the phase boundary between

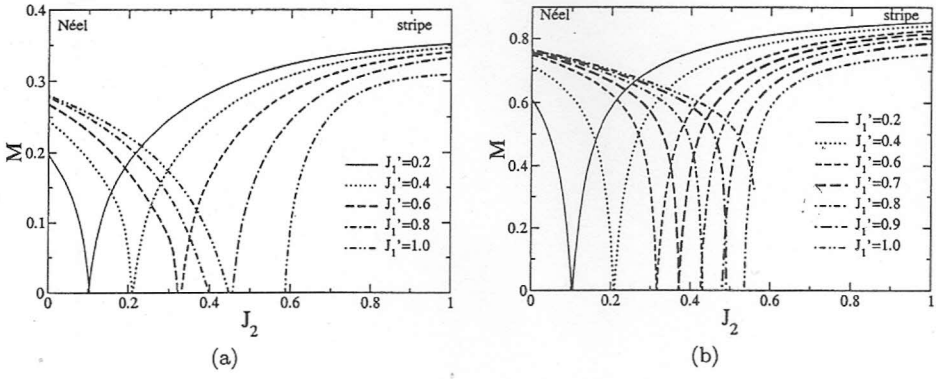

Fig. 3. Ground state staggered magnetization, M (with $J_1 = 1$): (a) for $s = 1/2$; and (b) for $s = 1$.

the quantum Néel and quantum stripe states. Thus, our definition of the quantum critical point is the point where there is an occurrence of a phase transition between the two states considered or where the order parameter vanishes, whichever occurs first.

For the $s = 1/2$ model we note that M vanishes for both the quantum Néel and stripe phases at almost exactly the same critical value of J_2, for a given J_1', so long as $J_1' \lesssim 0.6$. Conversely, for $J_1' \gtrsim 0.6$ there exists an intermediate region between the critical points at which $M \to 0$ for these two phases. The order parameters M of both the Néel and the stripe phases vanish continuously both below and above the point $J_1' \approx 0.60$, as is again typical of second-order transitions.

By contrast, we note the surprising result for the $s = 1$ model that the order parameter M goes to zero smoothly at the same point for both the quantum Néel and stripe phases with the same value of J_1', for all values of $J_1' \lesssim 0.66 \pm 0.03$, whereas the corresponding curves for the two phases meet at a nonzero value for higher values of J_1'. Thus, in this regime we have behaviour typical of a second-order phase transition between the quantum Néel and stripe phases. Furthermore, the transition occurs at a value of J_2 very close to the classical transition point at $J_2 = 0.5J_1'$. Conversely, for values of $J_1' \gtrsim 0.66 \pm 0.03$, the order parameters M of the two states meet at a finite value, as is typical of a first-order transition.

We show in Fig. 4 the zero-temperature phase diagrams of both the spin-1/2 and spin-1 J_1–J_1'–J_2 models on the square lattice, as obtained from our extrapolated results for both the GS energy and the GS order parameter M. In the case of the spin-1/2 model our results provide clear and consistent evidence for a *quantum triple point* (QTP) at ($J_1' \approx 0.60 \pm 0.03$, $J_2 \approx 0.33 \pm 0.02$) for $J_1 = 1$. For $J_1' \lesssim 0.60$ there exist only the Néel and stripe phases, with a second-order transition between them, whereas for $J_1' \gtrsim 0.60$ there also exists an intermediate (disordered, paramagnetic) quantum phase, which requires further investigation. Although the nature of the intermediate phase is still under discussion, a valence-bond crystal phase seems

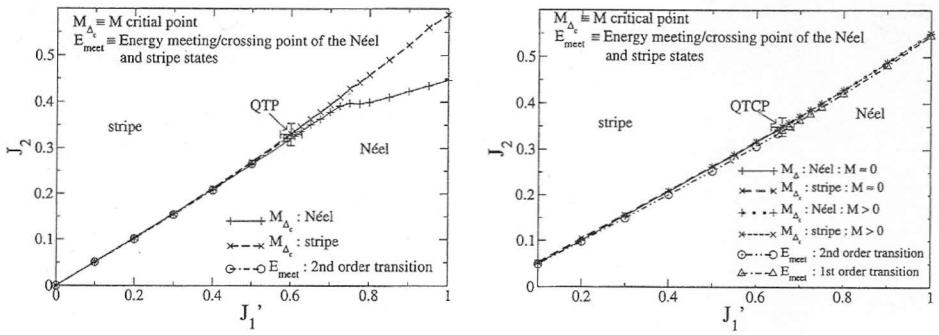

Fig. 4. Ground state phase diagrams (with $J_1 = 1$): (a) for $s = 1/2$, showing a quantum triple point (QTP); and (b) for $s = 1$, showing a quantum tricritical point (QTCP).

to be the most favoured from other investigations.[2,17] On the other hand, another possibility for this intermediate phase is the resonating valence bond (RVB) phase.[12] Other calculations on this spin-1/2 model[12,13] differ predominantly by giving a QTP at $(J_1' = 0, J_2 = 0)$ for $J_1 = 1$. We believe that the difference arises essentially from the nature of the alternative methods used. For example, due to the small size of the lattices used, the ED calculations of Sindzingre[12] might easily miss the longer-range correlations that become increasingly important the nearer one approaches the QTP.

Unlike the $s = 1/2$ case there is no sign at all of any intermediate disordered phase for any value of the parameters J_1' or J_2 (for $J_1 = 1$) for the case of $s = 1$. Hence, in this respect the quantum spin-1 model is much closer to the classical case, *viz.*, the $s \to \infty$ limit. However, unlike the classical case, there now appears to be a *quantum tricritical point* (QTCP) at $(J_1' \approx 0.66 \pm 0.03, J_2 \approx 0.35 \pm 0.02)$ for $J_1 = 1$, where a tricritical point is defined here to be a point at which a line of second-order phase transitions meets a line of first-order phase transitions. We note that the behaviour of both the order parameter (which goes to zero smoothly at the same point for both Néel and stripe phases below the QTCP, but which goes to a nonzero value above it) and the GS energy curves for the two phases (which meet smoothly with the same slope below the QTCP, but which cross with a discontinuity in slope above it) tell exactly the same story.

In conclusion we note that two of the unique strengths of the CCM are its ability to deal with highly frustrated systems as easily as unfrustrated ones, and its use from the outset of infinite lattices. These, in turn, lead to its ability to yield accurate phase boundaries even near quantum triple and tricritical points. Our own results for the ground state energy and staggered magnetization provide a set of independent checks that lead us to believe that we have a self-consistent and coherent description of these extremely challenging spin-1/2 and spin-1 systems.

References

1. P. Chandra and B. Doucot, *Phys. Rev. B* **38**, 9335 (1988).
2. J. Richter, *Phys. Rev. B* **47**, 5794 (1993); J. Richter, N.B. Ivanov, and K. Retzlaff, *Europhys. Lett.* **25**, 545 (1994).
3. H.J. Schulz, T.A.L. Ziman, and D. Poilblanc, *J. Phys. I* **6**, 675 (1996).
4. R.R.P. Singh, W.H. Zheng, J. Oitmaa, O.P. Sushkov and C.J. Hamer, *Phys. Rev. Lett.* **91**, 017201 (2003).
5. F. Krüger and S. Scheidl, *Europhysics Lett.* **74**, 896 (2006).
6. S. Moukouri, *Phys. Lett.* **A352**, 256 (2006).
7. D. Schmalfuß, R. Darradi, J. Richter, J. Schulenburg, and D. Ihle, *Phys. Rev. Lett.* **97**, 157201 (2006).
8. R. Melzi, P. Carretta, A. Lascialfari, M. Mambrini, M. Troyer, P. Millet, and F. Mila, *Phys. Rev. Lett.* **85**, 1318 (2000).
9. P. Carretta, N. Papinutto, C. B. Azzoni, M.C. Mozzati, E. Pavarini, S. Gonthier, and P. Millet, *Phys. Rev. B* **66**, 094420 (2002).
10. J. Richter, J. Schulenburg, and A. Honecker, in *Quantum Magnetism*, edited by U. Schollwöck, J. Richter, D.J.J. Farnell, and R.F. Bishop, *Lecture Notes in Physics*, Vol. **645**, (Springer-Verlag, Berlin, 2004), pp. 85–153.
11. A.A. Nersesyan and A.M. Tsvelik, *Phys. Rev. B* **67**, 024422 (2003).
12. P. Sindzingre, *Phys. Rev. B* **69**, 094418 (2004).
13. O.A. Starykh, and L. Balents, *Phys. Rev. Lett.* **93**, 127202 (2004).
14. S. Moukouri, *J. Stat. Mech.* P02002 (2006).
15. R. Darradi, J. Richter, and S.E. Krüger, *J. Phys.: Condens. Matter* **16**, 2681 (2004).
16. R. Darradi, J. Richter, and D.J.J. Farnell, *J. Phys.: Condens. Matter* **17**, 341 (2005).
17. J. Sirker, W.H. Zheng, O.P. Sushkov, and J. Oitmaa, *Phys. Rev. B* **73**, 184420 (2006).
18. T. Senthil, A. Vishwanath, L. Balents, S. Sachdev, and M.P.A. Fisher, *Science* **303**, 1490 (2004); T. Senthil, L. Balents, S. Sachdev, A. Vishwanath, and M.P.A. Fisher, *Phys. Rev. B* **70**, 144407 (2004).
19. R.F. Bishop, *Theor. Chim. Acta* **80**, 95 (1991).
20. R.F. Bishop in *Microscopic Quantum Many-Body Theories and Their Applications*, edited by J. Navarro and A. Polls, *Lecture Notes in Physics*, Vol. **510** (Springer-Verlag, Berlin, 1998), pp. 1–70.
21. D.J.J. Farnell and R.F. Bishop, in *Quantum Magnetism*, edited by U. Schollwöck, J. Richter, D.J.J. Farnell, and R.F. Bishop, *Lecture Notes in Physics*, Vol. **645** (Springer-Verlag, Berlin, 2004), pp. 307–348.
22. C. Zeng, D.J.J. Farnell, and R.F. Bishop, *J. Stat. Phys.* **90**, 327 (1998).
23. S.E. Krüger, J. Richter, J. Schulenburg, D.J.J. Farnell, and R.F. Bishop, *Phys. Rev. B* **61**, 14607 (2000).
24. D.J.J. Farnell, R.F. Bishop, and K.A. Gernoth, *J. Stat. Phys.* **108**, 401 (2002).
25. R. Darradi, J. Richter, and D.J.J. Farnell, *Phys. Rev. B* **72**, 104425 (2005).
26. D.J.J. Farnell, K.A. Gernoth, and R.F. Bishop, *Phys. Rev. B* **64**, 172409 (2001).
27. We use the program package CCCM of D.J.J. Farnell and J. Schulenburg, see http://www-e.uni-magdeburg.de/jschulen/ccm/index.html.
28. D.J.J. Farnell, J. Schulenburg, J. Richter, and K.A. Gernoth, *Phys. Rev. B* **72**, 172408 (2005).